Polarized bound state in the continuum and resonances with tunable Q-factor in an anisotropic photonic crystal

Ivan V. Timofeev[1,2,*], Dmitrii N. Maksimov[1,3], and Almas F. Sadreev[1]

[1]*Kirensky Institute of Physics, Federal Research Center KSC SB RAS, 660036, Krasnoyarsk, Russia*
[2]*Siberian Federal University, 660041, Kransnoyarsk, Russia*
[3]*Reshetnev Siberian State University of Science and Technology, 660037, Krasnoyarsk, Russia*
(Dated: October 19, 2017)

We consider a one-dimensional photonic crystal composed of alternating layers of isotropic and anisotropic dielectric materials. Such a system has different band structures for different polarizations of light. We demonstrate that if an anisotropic defect layer is inserted into the structure, the crystal can support an optical bound state in the continuum. By tilting the principle dielectric axes of the defect layer relative to those of the photonic crystal we observe a long-lived resonance in the transmission spectrum. We derive an analytical expression for the decay rate of the resonance that agrees well with the numerical data by the Berreman anisotropic transfer matrix approach. An experimental set-up with a liquid crystal defect layer is proposed to tune the Q-factor of the resonance through applying an external electric field. We speculate that the set-up provides a simple and robust platform for observing optical bound states in the continuum in the form of resonances with tunable Q-factor.

I. INTRODUCTION

The spectral properties of open systems are characterized by resonant eigenvalues, which are typically complex numbers. It is generally perceived that the imaginary part of a resonant eigenvalue is due to the coupling of the resonant state to the continuum of propagating eigenmodes corresponding to the scattering channels. It might occurs, however, that under variation of some parameters the imaginary part of a resonant eigenvalue tends to zero, i.e. the resonant state becomes decoupled from the scattering channels, whilst still embedded into the spectrum of the extended states. Such continuum decoupled states are source-free localized eigenmodes with infinite lifetime known as bound states in the continuum (BICs)[1].

The symmetry selection rules provide the simplest mechanism for cancelling the coupling of a bound state to the continuum. The symmetry protected BICs in quantum waveguides were first proposed by Robnik in a simple separable system with antisymmetric BICs embedded into the spectrum of symmetric propagating eigenstates[2]. Later on the symmetry protected BICs were reported in a cross-wire waveguide[3] and a quantum dot subject to magnetic field[4].

Nowadays we witness a surge of interest to BICs in field of photonics, where BICs were observed in various set-ups with periodical dielectric permittivity[5–10]. In particular, the studies on BICs are motivated by applications to resonant light enhancement[11–13] and lasing[14,15]. Another remarkable property of BICs is the emergence of a collapsing Fano feature in its parametric vicinity[16–19], that can be potentially employed to narrow-band filters[20,21]. To the best of our knowledge, optical resonances with infinite lifetime in the Γ-point (i.e. symmetry protected BICs) were first predicted in[22]. Another optical set-up supporting symmetry protected BICs is a di-

rectional waveguide side-coupled with two off-channel microcavities[23] buried in the bulk of a two-dimensional photonic crystal (PhC). That is the set-up experimentally realized by Plotnik *et al*[5]. Recently, BICs have been studied in systems with dielectric anisotropy[24,25] with the key idea to employ the anisotropy for manipulating the frequency cut-offs for different polarizations of light in the ambient medium.

In this paper we propose a simple set-up for a symmetry protected BIC localized in the vicinity of an anisotropic defect layer (ADL) embedded into a one-dimensional anisotropic PhC. The proposed set-up is similar to that from[24] with the only difference that the defect layer in the above reference was taken isotropic. We will show that the addition of an ADL allows us to provide an exact analytical solution for a BIC and derive the decay rate of the BIC related resonance in the transmission/reflection spectra. An experimental set-up with a liquid crystal ADL is proposed to control the Q-factor through applying an external electric field.

The paper is organized as follows: in Sec. II we review the band structure of anisotropic PhCs, describe our model, and numerically demonstrate the resonant feature associated with a BIC. In Sec. III we present an exact analytical solution for the BIC within the extraordinary waves stop-band. In Sec. IV we derive the decay rate of BIC-related resonance which emerges in the scattering spectrum when the symmetry is broken by application of ADL axes tilt. We confirm our findings with numerical data in Sec. V. Finally, we conclude in Sec. VI.

II. MODEL

We consider a one-dimensional PhC composed of alternating layers of isotropic and anisotropic dielectric mate-
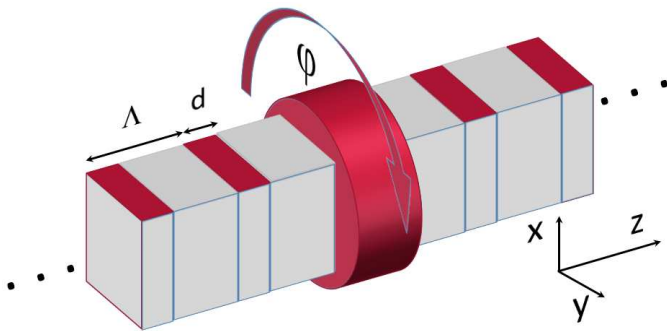
FIG. 1. One-dimensional PhC structure stacked of alternating layers of an isotropic dielectric material with permittivity ϵ_o (gray) and an anisotropic material with the permittivity components ϵ_o and ϵ_e (red). A defect layer with a tuneable permittivity tensor is inserted in the center of the structure.

rials as shown in Fig. 1. The layers are stacked along the z-axis with period Λ. The isotropic layers are made of a dielectric material with permittivity ϵ_o and thickness $\Lambda - d$, while the anisotropic layers have the principal dielectric axes aligned with the x,y-axes with the corresponding permittivity components ϵ_e, ϵ_o. The thickness of each anisotropic layer is d.

We start with Maxwell's equations for waves propagating along the z-axis. Assuming that the wave vector is aligned with the z-axis the wave equations for the electric vector $\mathbf{E} = [E_x, E_y, 0]$ are the following

$$\frac{\partial^2 E_x}{\partial z^2} + \frac{\omega^2}{c^2}\epsilon_o E_x = 0,$$
$$\frac{\partial^2 E_y}{\partial z^2} + \frac{\omega^2}{c^2}\epsilon(z) E_y = 0, \tag{1}$$

where $\epsilon(z)$ is either ϵ_o within the isotropic layer, or ϵ_e within the anisotropic ones. The solution for the ordinary y-polarized waves is obvious

$$E_y = E_0 \exp\left(in_o k_0 z - i\omega t\right), \tag{2}$$

where $k_0 = \omega/c$ is the wave vector in vacuum, while $n_o = \sqrt{\epsilon_o}$ is the refractive index of the isotropic material. For the extraordinary x-polarized waves we have a piecewise continuus solution. By using the transfer matrix approach the dispersion relation for the extraordinary waves is found as[26,27]

$$\cos k_B \Lambda = \cos k_e d \ \cos k_0(\Lambda - d) -$$
$$\frac{1}{2}\left(\frac{n_e}{n_o} + \frac{n_o}{n_e}\right)\sin k_e d \ \sin k_0(\Lambda - d),$$

where $k_e = (\omega/c)\sqrt{\epsilon_e}$, $n_e = \sqrt{\epsilon_e}$, and k_B is the Bloch vector. The band structure is shown in Fig.2(left).

According to Eq. (1) the waves of different polarization do not mix in the PhC structure. The picture becomes more involved if an anisotropic defect layer (ADL) of thickness $2d$ is inserted into the center of the structure.

In what follows we assume that the ADL is made of a material with the same principal dielectric constants ϵ_o, ϵ_e, but the principal axes of the ADL are tilted with respect of the principle axes of the bulk PhC by angle ϕ as shown in Fig. 1. We mention in passing that the set-up could be implemented with a liquid crystal defect layer with the principal axes aligned with an external electric field. The dielectric tensor of the ADL can be written as

$$\hat{\epsilon} = \left[\begin{array}{cc} \epsilon_e \cos^2\phi + \epsilon_o \sin^2\phi & \sin 2\phi \ (\epsilon_e - \epsilon_o)/2 \\ \sin 2\phi \ (\epsilon_e - \epsilon_o)/2 & \epsilon_e \sin^2\phi + \epsilon_o \cos^2\phi \end{array}\right], \tag{3}$$

where the tilt angle ϕ is the polar angle in the $x0y$-plane. For brevity here and later on we omit the z-components the electromagnetic (EM) field, since $\hat{\epsilon}$ is a 2×2 matrix.

The whole system can be now viewed as a one-dimensional scattering set-up with the ADL playing the role of the scattering center and the PhC arms acting as semi-infinite waveguides. The resonant properties of the system can be probed by an ordinary wave Eq. (2) injected through the left arm. It is clear from Eq. (3) that if $\phi = 0$ the system remains transparent for the incident wave Eq. (2). If, however, a tilt $\phi \neq 0$ of the dielectric axes is applied to the ADL we expect a scattering solution with a mixture of both polarizations in the vicinity of the ADL. The above speculation is exemplified with numerical results in Fig. 2 (right). The numerical data are obtained with the Berreman transfer matrix method[28] for the set of parameters collected in the caption to Fig. 2. Most remarkably, one can see from Fig. 2 that the reflectance spectrum of the ordinary wave exhibits a resonant feature in the middle of the extraordinary waves stop-band. In what follows we will demonstrate that this feature is induced by an x-polarized BIC which is converted to a long-lived resonance (quasi-BIC) by the ADL axes tilt.

III. BOUND STATE IN THE CONTINUUM

Let us now construct a BIC solution for the ADL. By definition the BIC is a source free solution localized in the vicinity of the ADL. The solution must satisfy time-stationary Maxwell's equations

$$\left\{\begin{array}{cc} 0 & \nabla\times \\ -\nabla\times & 0 \end{array}\right\}\left\{\begin{array}{c} \mathbf{E} \\ \mathbf{H} \end{array}\right\} = -ik_0\left\{\begin{array}{c} \hat{\epsilon}\mathbf{E} \\ \mathbf{H} \end{array}\right\}, \tag{4}$$

where $k_0 = \omega/c$. Let us take the layers of equal quarter-wavelength optical thickness for both materials

$$dn_e = (\Lambda - d)n_o = \lambda_0/4, \tag{5}$$

with $\lambda_0 = 2\pi/k_0$ as the vacuum wavelength. Notice that the above choice of parameters constraints both the angular frequency of the BIC
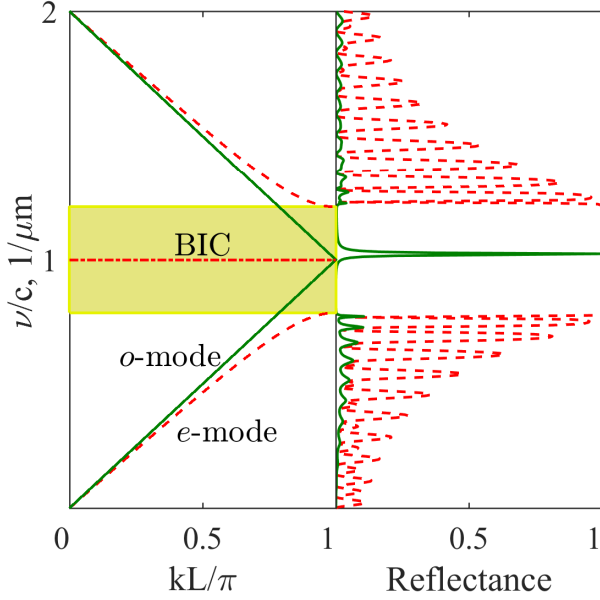
$$\omega = \frac{c\pi}{2dn_e}, \tag{6}$$

FIG. 2. The band structure (left) and reflectance spectra (right) of extraordinary (dash red) and ordinary waves (solid green) in anisotropic PhC structure from Fig. 1 with ν as the linear frequency of the incident wave. The BIC frequency is marked by a red dash-dot line. The yellow strip is the photonic band gap. Dielectric permittivities of layers are $\epsilon_e = 4; \epsilon_o = 1$. The widths $d = 0.125\,\mu m$, $(\Lambda - d) = 0.250\,\mu m$ are optimized for normalized linear frequency $\nu/c = 1/\lambda = 1\,\mu m^{-1}$ in the band gap center. The defect layer has twice the thickness of the anisotropic layers $2d = 0.250\,\mu m$. The tilt angle $\phi = \pi/8$.

and the period of the PhC

$$\Lambda = \frac{d(n_e + n_o)}{n_o}. \tag{7}$$

In what follows we show that the specific choice of parameters given by Eqs.(5,6,7) allows us to construct a source-free solution that exponentially decays away from the ADL. In the unperturbed case $\phi = 0$ the BIC is polarized along the x-axis, hence for the EM field within the ADL we can write

$$\begin{aligned}
E_x^{(0)}(z) &= \frac{1}{n_e} A \sin(n_e k_0 z), \\
H_y^{(0)}(z) &= -iA \cos(n_e k_0 z).
\end{aligned} \tag{8}$$

The above solution obviously satisfies Eq. (4) within the ADL. Let us demonstrate that it can be extended into the PhC arms by matching the EM fields on the boundaries between the anisotropic and isotropic layers. We denote the EM field components in the isotropic layers adjacent to the ADL by $\bar{E}_x^{(0)}(z)$, and $\bar{H}_y^{(0)}(z)$. On the boundaries of the ADL the following boundary conditions must be satisfied

$$\bar{E}_x^{(0)}(\pm d) = E_x^{(0)}(\pm d), \ \ \bar{H}_y^{(0)}(\pm d) = H_y^{(0)}(\pm d). \tag{9}$$

Here we describe the wave matching for $z > 0$ having in mind that by construction the solution Eq. (8) is anti-

symmetric with respect to the z-axis. By using Eq. (8) we can write

$$\begin{aligned}
\bar{E}_x^{(0)}(z) &= \frac{1}{n_e} A \sin[n_o k_0 (\Lambda - z)], \\
\bar{H}_y^{(0)}(z) &= iqA \cos[n_o k_0 (\Lambda - z)],
\end{aligned} \tag{10}$$

where

$$q = \frac{n_o}{n_e} < 1.$$

Re-iterating the matching procedure into the depth of the PhC arm we find the EM fields within the m_{th} anisotropic and isotropic layers

$$\begin{aligned}
E_x^{(m)}(z) &= \frac{1}{n_e}(-1)^m q^m A \sin[n_e k_0 (z - m\Lambda)], \\
H_y^{(m)}(z) &= i(-1)^{m+1} q^m A \cos[n_e k_0 (z - m\Lambda)],
\end{aligned} \tag{11}$$

and

$$\begin{aligned}
\bar{E}_x^{(m)}(z) &= \frac{1}{n_e}(-1)^m q^m A \sin[n_o k_0 ((m+1)\Lambda - z)], \\
\bar{H}_y^{(m)}(z) &= i(-1)^m q^{m+1} A \cos[n_o k_0 ((m+1)\Lambda - z)].
\end{aligned} \tag{12}$$

One can see that we have found a localized solution which decays exponentially with m, Q.E.D.

Let us define the quantities $\mathcal{E}_m$, $\bar{\mathcal{E}}_m$ as the energies stored in the $m_{\text{th}}, m = 0, 1, 2, \ldots$ anisotropic and isotropic layers, correspondingly. Notice that for $\phi = 0$ one half of the ADL $m = 0$ is identical to the next anisotropic layers in the PhC arm $m = 1, 2, \ldots$. The energies can be expressed through the integrals

$$\mathcal{E}_m = \frac{1}{8\pi} \int_{m\Lambda}^{m\Lambda + d} dz \left[\mathbf{E}^{(m)\,\dagger} \hat{\epsilon}(z) \mathbf{E}^{(m)} + \mathbf{H}^{(m)\,\dagger} \mathbf{H}^{(m)} \right], \tag{13}$$

and

$$\bar{\mathcal{E}}_m = \frac{1}{8\pi} \int_{m\Lambda + d}^{(m+1)\Lambda} dz \left[\bar{\mathbf{E}}^{(m)\,\dagger} \hat{\epsilon}(z) \bar{\mathbf{E}}^{(m)} + \bar{\mathbf{H}}^{(m)\,\dagger} \bar{\mathbf{H}}^{(m)} \right]. \tag{14}$$

The integrals can be evaluated as

$$\mathcal{E}_m = \frac{dA^2 q^{2m}}{8\pi}, \ \ \bar{\mathcal{E}}_m = \frac{(\Lambda - d)A^2 q^{2m+2}}{8\pi} = \frac{dA^2 q^{2m+1}}{8\pi}, \tag{15}$$

where Eq. (5) was used in the last step of the derivation. The total energy stored in the BIC is, then, expressed through the following equation

$$\mathcal{E} = 2\sum_{m=0}^{\infty} (\mathcal{E}_m + \bar{\mathcal{E}}_m) = \frac{dA^2}{4\pi(1-q)}. \tag{16}$$

By equating the total energy to unity we have

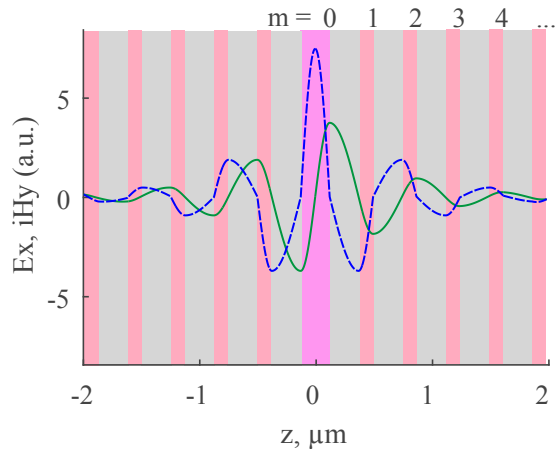$$A = \sqrt{\frac{4\pi(1-q)}{d}}. \tag{17}$$

FIG. 3. BIC mode profile; The electric field E_x – solid green, the magnetic field H_y – dash blue; tilt angle $\phi = \pi/18$. The other parameters are the same as in Fig. 2.

One can see that the BIC is now energy normalized in the whole space for any value of the parameters $d, \epsilon_o, \epsilon_e$.

The BIC mode profile is plotted in Fig. 3. Notice, that the structure is simmetric with respect to $x0z$- and $y0z$-plane mirror reflections. The BIC polarization is orthogonal to the polarization of propagating waves Eq. (2). This orthogonality can be thought of as a case of symmetry protection.

IV.   DECAY RATE

As it was demonstrated in Sec. II, in case the principle axes of the ADL are tilted by angle $\phi \neq 0$ the BIC becomes a leaky mode (quasi-BIC) emerging in the reflection spectrum as a sharp resonant feature. In this section we derive an analytical expression for the energy decay rate Γ which by definition is the ratio of the power lost into the continuum of the ordinary waves, P to the energy stored in the BIC, $\mathcal{E}$

$$\Gamma = \frac{\mathcal{P}}{\mathcal{E}}. \tag{18}$$

Taking into account that the BIC is energy normalized the only unknown quantity in Eq. (18) is $\mathcal{P}$. Next we will demonstrate how two different techniques could be used for finding $\mathcal{P}$.

A.   Wave matching

We start with a heuristical wave-matching approach, similar in spirit to that from[29–31]. Let us consider the standing wave solution in the ADL inserted to the isotropic medium of adjacent layers. In the considered case the ADL produces no reflection for stationary incident waves of arbitrary polarization. The ordinary wave is not reflected because of matched impedances with equal dielectric permittivity. For the extraordinary wave the ADL is a half-wavelength layer according to Eq. (5). The total reflection from both boundaries of a half-wavelength layer is zero, see Eqs. (8) and (10) and Fig. 3 with the electric field maximum at the ADL boundary. So, the electric field amplitude inside the ADL and in the adjacent layers is the same. Thus, the leakage is due to transmission rather than reflection.

The standing wave can be decomposed into incident and outgoing waves with respect to the ADL with electric field amplitudes $A_{(\mp)}$

$$A_{(\mp)} = \frac{1}{n_e} \sqrt{\frac{\pi(1-q)}{d}}.$$

One can write the matching condition with ordinary and extraordinary waves within the tilted ADL

$$\begin{aligned} E_e(-d) &= A_{(+)} \cos\phi \\ E_o(-d) &= A_{(+)} \sin\phi, \end{aligned} \tag{19}$$

where E_e, and E_o are the amplitudes of ordinary and extraordinary waves propagating to the right within the ADL at the left interface $z = -d$. After propagating to the right interface $z = d$ those waves accumulate phase

$$E_{e,o}(d) = E_{e,o}(-d) \exp(2idn_{e,o}k_0). \tag{20}$$

Projecting back onto the y-axis and combining the above equations (19) and (20) we have for the amplitude of the outgoing wave in the right PhC arm

$$|E_y| = \frac{1}{n_e} \sqrt{\frac{\pi(1-q)}{d}} \sin(2\phi) \sin\left(dk_0(n_e - n_o)\right). \tag{21}$$

Then, the Poynting vector amplitude of the outgoing wave can be written as

$$P = cn_o|E_y^2|/4\pi. \tag{22}$$

The total energy loss must be obviously doubled to account for leakage into the left PhC arm. Hence, by using Eqs. (6,21) and (22) we have for the power lost in unit of time

$$\mathcal{P} = \frac{c\sin(2\phi)^2 q^2(1-q)}{2dn_o} \cos^2\left(\frac{\pi q}{2}\right). \tag{23}$$

At this point we would like to emphasise the obvious violation of a half-wavelength condition Eq. (5) by the ADL tilt. When the tilt is small the quasi-BIC frequency shift is proportional to ϕ^2, and the residual reflection amplitude has the same order of smallness. Then the reflection amplitude projection onto the y-axis is proportional to ϕ^3. Thus, the expression Eq. (23) is accurate up to $\mathcal{O}(\phi^4) \sim \phi^3 sin(2\phi)$.

B. Time-dependant perturbation theory

To obtain an analytical expression for $\mathcal{P}$ in a more rigorous manner we will apply the time-dependant perturbation theory assuming that initially the EM energy is loaded into the BIC with $\phi = 0$. Then, at the moment $t = 0$ an axes tilt is applied to the system, and the energy stored in the BIC leaks into the continuum of the ordinary waves. Expanding the dielectric tensor in the powers of ϕ one finds

$$\hat{\epsilon}(z,t) = \hat{\epsilon}_0(z) + \theta(t)\theta(d - |z|)\hat{\epsilon}_1 + \mathcal{O}(\phi^2), \qquad (24)$$

where $\hat{\epsilon}_0(z)$ is the dielectric tensor of the unperturbed system, $\theta(\ldots)$ - the Heaviside step function, and $\hat{\epsilon}_1$ can be found from Eq. (3) as

$$\hat{\epsilon}_1 = -\phi\epsilon_e \left\{ \begin{array}{cc} 0 & 1 - q^2 \\ 1 - q^2 & 0 \end{array} \right\}. \qquad (25)$$

Using the notation

$$\hat{H} = \left\{ \begin{array}{cc} 0 & \nabla\times \\ -\nabla\times & 0 \end{array} \right\} \qquad (26)$$

we can write temporal Maxwell's equations

$$\hat{H}\mathbf{\Psi}(t) = \frac{\partial}{\partial t}\left\{[\hat{\epsilon}_0(z) + \theta(t)\theta(d - |z|)\hat{\epsilon}_1]\mathbf{\Psi}(t)\right\}, \qquad (27)$$

where $\mathbf{\Psi}$ is 4×1 vector $\mathbf{\Psi} = [E_x, E_y, H_x, H_y]$. To proceed we write the solutions of the continuous spectrum as

$$\mathbf{\Psi}(k,z) = [0, E_y(k,z), H_x(k,z), 0] \qquad (28)$$

with

$$\begin{array}{l} E_y(k,z) = \sqrt{\frac{2}{n_o}}e^{in_o kz}, \\ H_x(k,z) = \sqrt{2n_o}e^{in_o kz}. \end{array} \qquad (29)$$

The solutions are normalized to the Dirac delta

$$\frac{1}{8\pi}\int_{-\infty}^{\infty}\mathbf{\Psi}(k,z)^{\dagger}\hat{\epsilon}_0(z)\mathbf{\Psi}(k',z)dz = \delta(k - k').$$

Now we have all necessary ingredients for the time-dependant perturbation theory[32] at our disposal. According to the first order time-dependant perturbation theory the solution is given by

$$\mathbf{\Psi}(t,z) = \mathbf{\Psi}_0(z)e^{-ick_0 t} + \int_{-\infty}^{\infty}b(k,t)\mathbf{\Psi}(k,z)e^{-ic|k|t} + \mathcal{O}(\phi^2), \qquad (30)$$

where $b(k,t) \sim \phi$, and $\mathbf{\Psi}_0(z)$ is the BIC mode profile. After substituting the above into Eq. (27) we find

$$\frac{\partial b(k,t)}{\partial t} = [\delta(t) - ick_0\theta(t)]e^{ic(|k| - k_0)t}V(k) \qquad (31)$$

with

$$V(k) = \int_{-d}^{d}dz\mathbf{\Psi}^{\dagger}(k,z)\hat{\epsilon}_1\mathbf{\Psi}_{(0)}(z). \qquad (32)$$

Evaluating the above integral we have

$$V(k) = -(1 - q^2)n_e\phi\sqrt{\frac{1 - q}{8\pi n_0 d}}f(k,k_0), \qquad (33)$$

where

$$f(k,k_0) = \frac{\sin[d(n_o k - n_e k_0)]}{n_o k - n_e k_0} - \frac{\sin[d(n_o k + n_e k_0)]}{n_o k + n_e k_0}. \qquad (34)$$

The energy lost to the continuum per unit of time can be now found as

$$\mathcal{P}(t) = \frac{1}{8\pi}\frac{\partial}{\partial t}\int_{-\infty}^{\infty}dz\left[\mathbf{\Psi}^{\dagger}(t)\hat{\epsilon}_0\mathbf{\Psi}(t)\right]. \qquad (35)$$

Notice that the $\mathcal{P}(t)$ is time-dependant. Hence, we define time-averaged energy loss in the following manner

$$\mathcal{P} = \lim_{T\to\infty}\frac{1}{T}\int_0^T dt\mathcal{P}(t).$$

The above definition may appear superfluous, however, by subsisting into it Eqs. (35) and (27) and applying the normalization condition we find a useful expression that will eventually simplify the further analysis

$$\mathcal{P} = \lim_{T\to\infty}\frac{1}{T}\int_0^T dt\int_{-\infty}^{\infty}dk\left(b^*(k)\frac{\partial b(k)}{\partial t} + \frac{\partial b^*(k)}{\partial t}b(k)\right) + \mathcal{O}(\phi^4), \qquad (36)$$

where the terms $\mathcal{O}(\phi^3)$ are dropped off since $\mathcal{P}$ is symmetric with respect to the sign of ϕ. Substituting Eq. (31) into Eq. (36) and using L'Hopital's rule one obtains

$$\mathcal{P} = [(1 - q^2)ck_0\phi]^2\frac{n_e^2(1 - q)}{4\pi n_o d}\times$$

$$\lim_{T\to\infty}\int_0^T dt\int_{-\infty}^{\infty}dk\cos[tc(k_0 - |k|)]f(k,k_0)^2 + \mathcal{O}(\phi^4). \qquad (37)$$

By recollecting the identity

$$\delta(x - x') = \frac{1}{\pi c}\int_0^{\infty}dt\cos[tc(x - x')]$$

we obtain

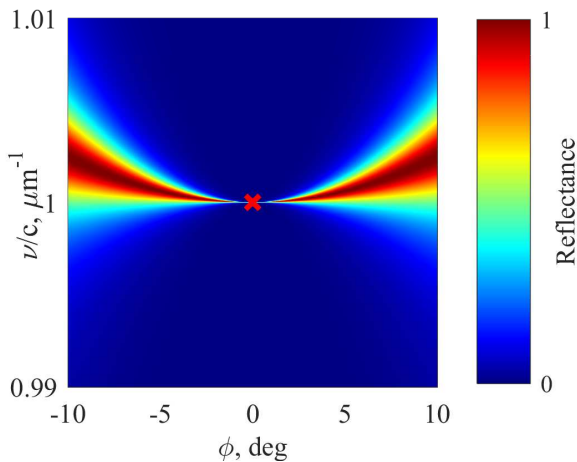$$\mathcal{P} = [(1 - q^2)k_0\phi]^2\frac{cn_e^2(1 - q)}{2n_o d}f(k_0, k_0)^2 + \mathcal{O}(\phi^4). \qquad (38)$$

FIG. 4. Reflectance $|\rho|^2$ versus tilt angle ϕ and linear frequency ν. The other parameters are the same as in Fig. 1. The red cross in the center corresponds to the BIC.

Next by using Eq. (6) we have

$$
\begin{aligned}
f(k_0, k_0)^2 &= \frac{1}{k_0^2 n_e^2} \left\{ \frac{\sin\left[(1-q)\frac{\pi}{2}\right]}{1-q} - \frac{\sin\left[(1+q)\frac{\pi}{2}\right]}{1+q} \right\}^2 \\
&= \frac{4q^2}{k_0^2 n_e^2 (1-q^2)^2} \cos^2\left(\frac{\pi q}{2}\right)
\end{aligned} \tag{39}
$$

and finally

$$
\mathcal{P} = \frac{2c\phi^2 q^2 (1-q)}{dn_o} \cos^2\left(\frac{\pi q}{2}\right) + \mathcal{O}(\phi^4). \tag{40}
$$

One can see that Eqs. (23) and (40) differ by $\mathcal{O}(\phi^4)$.

V. NUMERICAL RESULTS

In this section we establish a link between the decay rate Γ, Eq. (18) and the numerical data on the transmission and reflection spectra. The scattering problem under consideration poses a typical case of two pathways transmission problem, where the direct path is identified with the incident ordinary wave penetrating through the ADL from the left to the right PhC arm. The second pathway is through the resonant excitation of the quasi-BIC. Such scattering problem was thoroughly analyzed by Suh, Wang, and Fan[33] in the framework of the Coupled Mode Theory[34]. The general expression for the reflection/transmission amplitudes was obtained as

$$
\rho = \frac{i\gamma}{(\omega_r - \omega) + i\gamma}, \quad \tau = 1 - \rho, \tag{41}
$$

where ω_r is the position of the resonance, and γ is the imaginary part of the resonant frequency. Remarkably, the transmission amplitude τ exhibits a transmission zero at $\omega = \omega_r$ which could be understood as a consequence of a full destructive interference between the two transmission pathways. On the other hand, the reflection amplitude ρ is simply a Lorentzian of the width 2γ. Taking
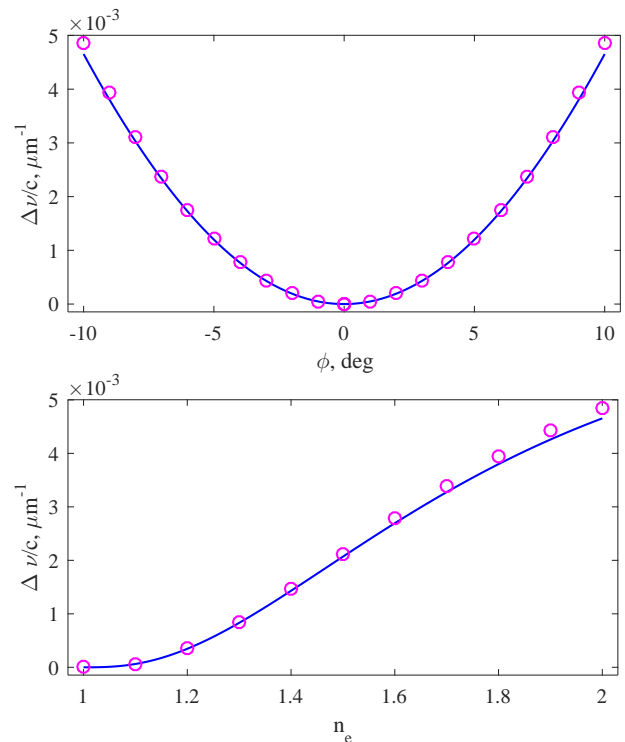

FIG. 5. Resonance width $\Delta\nu$ vs. tilt angle ϕ for $n_e = 2$ (top), and the refraction index n_e for $\phi = \pi/18$ (bottom). The geometry of the system is the same as in Fig. 1. The numerical data are shown by red circles, the analytical results obtained from Eq. (23) are shown by blue solid line.

into account that the energy relaxation time of a resonant state is given by

$$
\Gamma = 2\gamma,
$$

we find a link between Eqs. (18,23) and (40), and the resonant width in the reflection spectrum as

$$
\Delta\nu = \frac{\gamma}{\pi}, \tag{42}
$$

where ν is the linear frequency.

In Fig. 4 we present the reflectance vs. the tilt angle ϕ and linear frequency of the incident wave ν. In the BIC point we observe a collapse of the resonance as its width turns to zero. The numerical data from Fig. 4 were used for comparing the resonance widths with our analytical predictions. The results are shown in Fig. 5, where one can see a good agreement between theory and numerical experiment.

VI. CONCLUSION

Most of theoretical works on PhCs rely on various numerical techniques[23,25,35–37] for finding BIC frequencies and mode profiles. So far, to the best of our knowledge, the only model with analytical solution for

optical BICs was photonic Lieb lattice[8,38]. Here we have found an exact analytical solution for an optical BIC in an anisotropic defect layer embedded into an anisotropic PhC. Moreover, the decay rate of a qausi-BIC resonance in the system with tilted principal axes of the defect layer was computed with the use of the time-dependant perturbation theory and the transmission/reflection spectra are explained through the coupled mode approach. A simple experimental set-up with a liquid crystal defect layer is proposed to tune the Q-factor through applying an external low-frequency electric field. The question of BICs tunability has been previously discussed in the literature[39] with the optical properties of the system changing under variation of the thickness of dielectric slabs. This approach, how-ever, would require re-fabrication of the BIC supporting structure. The idea of using the optoelectronic effect for manipulating the Q-factor has already been applied to liquid metacrystals[40,41] and microring resonantors[42–44]. We speculate that the analytical approaches proposed in this work may find application to various set-ups with optoelectronically controlled Q-factors.

* tiv@iph.krasn.ru
[1] C. W. Hsu, B. Zhen, A. D. Stone, J. D. Joannopoulos, and M. Soljačić, Nat. Rev. Mater. 1, 16048 (2016).
[2] M. Robnik, J. Phys. A Math. Gen. 19, 3845 (1986).
[3] R. L. Schult, D. G. Ravenhall, and H. W. Wyld, Phys. Rev. B 39, 5476 (1989).
[4] J. U. Nöckel, Phys. Rev. B 46, 15348 (1992).
[5] Y. Plotnik, O. Peleg, F. Dreisow, M. Heinrich, S. Nolte, A. Szameit, and M. Segev, Phys. Rev. Lett. 107, 28 (2011).
[6] S. Weimann, Y. Xu, R. Keil, A. E. Miroshnichenko, A. Tünnermann, S. Nolte, A. A. Sukhorukov, A. Szameit, and Y. S. Kivshar, Phys. Rev. Lett. 111, 240403 (2013).
[7] C. W. Hsu, B. Zhen, J. Lee, S.-L. Chua, S. G. Johnson, J. D. Joannopoulos, and M. Soljačić, Nature 499, 188 (2013).
[8] R. A. Vicencio, C. Cantillano, L. Morales-Inostroza, B. Real, C. Mej\'\ia-Cortés, S. Weimann, A. Szameit, and M. I. Molina, Phys. Rev. Lett. 114, 245503 (2015).
[9] Z. F. Sadrieva, I. S. Sinev, K. L. Koshelev, A. Samusev, I. V. Iorsh, O. Takayama, R. Malureanu, A. A. Bogdanov, and A. V. Lavrinenko, ACS Photonics 4, 723 (2017).
[10] Y.-X. Xiao, G. Ma, Z.-Q. Zhang, and C. Chan, Phys. Rev. Lett. 118, 166803 (2017).
[11] V. Mocella and S. Romano, Phys. Rev. B 92, 155117 (2015).
[12] J. W. Yoon, S. H. Song, and R. Magnusson, Sci. Rep. 5, 18301 (2015).
[13] E. N. Bulgakov and D. N. Maksimov, Opt. Express 25, 14134 (2017).
[14] A. Kodigala, T. Lepetit, Q. Gu, B. Bahari, Y. Fainman, and B. Kanté, Nature 541, 196 (2017).
[15] B. Bahari, F. Vallini, T. Lepetit, R. Tellez-Limon, J. H. Park, A. Kodigala, Y. Fainman, and B. Kante, "Integrated and Steerable Vortex Lasers using Bound States in Continuum," (2017), arXiv:1707.00181.
[16] C. S. Kim, A. M. Satanin, Y. S. Joe, and R. M. Cosby, Phys. Rev. B 60, 10962 (1999).
[17] S. P. Shipman and S. Venakides, Phys. Rev. E 71, 26611 (2005).
[18] A. F. Sadreev, E. N. Bulgakov, and I. Rotter, Phys. Rev. B 73, 235342 (2006).
[19] C. Blanchard, J.-P. Hugonin, and C. Sauvan, Phys. Rev. B 94, 155303 (2016).
[20] J. M. Foley, S. M. Young, and J. D. Phillips, Phys. Rev. B 89, 165111 (2014).
[21] X. Cui, H. Tian, Y. Du, G. Shi, and Z. Zhou, Sci. Rep. 6, 36066 (2016).
[22] V. Pacradouni, W. J. Mandeville, A. R. Cowan, P. Paddon, J. F. Young, and S. R. Johnson, Phys. Rev. B 62, 4204 (2000).
[23] E. N. Bulgakov and A. F. Sadreev, Phys. Rev. B 78, 75105 (2008).
[24] S. P. Shipman and A. T. Welters, J. Math. Phys. 54, 103511 (2013).
[25] J. Gomis-Bresco, D. Artigas, and L. Torner, Nat. Photonics 11, 232 (2017).
[26] P. Markoš and C. M. Soukoulis, Wave Propagation: From Electrons to Photonic Crystals and Left-Han (Princeton University Press, 2008).
[27] A. Yariv and P. Yeh, Photonics: Optical Electronics in Modern Commu The Oxford series in electrical and computer engineering (Oxford University Press, 2007).
[28] D. W. Berreman, J. Opt. Soc. Am. 62, 502 (1972).
[29] M. Becchi, S. Ponti, J. A. Reyes, and C. Oldano, Phys. Rev. B 70, 33103 (2004).
[30] V. A. Belyakov and S. V. Semenov, J. Exp. Theor. Phys. 112, 694 (2011).
[31] I. V. Timofeev, P. S. Pankin, S. Y. Vetrov, V. G. Arkhipkin, W. Lee, and V. Y. Zyryanov, Crystals 7, 113 (2017), arXiv:1703.00310.
[32] L. D. Landau and E. M. Lifshitz, Quantum Mechanics: Non-relativistic Theory. V. 3 of Course of Theo (Pergamon Press, 1958).
[33] W. Suh, Z. Wang, and S. Fan, IEEE J. Quantum Electron. 40, 1511 (2004).
[34] C. Manolatou, M. J. Khan, S. Fan, P. R. P. Villeneuve, H. A. Haus, and J. D. Joannopoulos, IEEE J. Quantum Electron. 35, 1322 (1999).
[35] S. Venakides and S. P. Shipman, SIAM J. Appl. Math. 64, 322 (2003).
[36] D. C. Marinica, A. G. Borisov, and S. V. Shabanov, Phys. Rev. Lett. 100, 183902 (2008).
[37] X. Gao, C. W. Hsu, B. Zhen, X. Lin, J. D. Joannopoulos, M. Soljačić, and H. Chen, Sci. Rep. 6, 31908 (2016).

[38] J. Mur-Petit and R. A. Molina, Phys. Rev. B **90**, 035434 (2014).

[39] L. Ni, Z. Wang, C. Peng, and Z. Li, Phys. Rev. B **94**, 245148 (2016).

[40] A. Piccardi, A. Alberucci, N. Kravets, O. Buchnev, and G. Assanto, Nat. Commun. **5**, 5533 (2014).

[41] A. A. Zharov, A. A. Zharov, and N. A. Zharova, Phys. Rev. E **90**, 23207 (2014).

[42] T.-J. Wang, C.-H. Chu, and C.-Y. Lin, Opt. Lett. **32**, 2777 (2007).

[43] A. Guarino, G. Poberaj, D. Rezzonico, R. Degl-Innocenti, and P. Gunter, Nat. Photonics **1**, 407 (2007).

[44] C.-T. Wang, Y.-C. Li, J.-H. Yu, C. Y. Wang, C.-W. Tseng, H.-C. Jau, Y.-J. Chen, and T.-H. Lin, Opt. Express **22**, 17776 (2014).